

# Mechanistic Aspects of the Electroreduction of Dioxygen As Catalyzed by Copper–Phenanthroline Complexes Adsorbed on Graphite Electrodes

Yabin Lei and Fred C. Anson\*

Arthur Amos Noyes Laboratories, Division of Chemistry and Chemical Engineering,<sup>§</sup> California Institute of Technology, Pasadena, California 91125

Received May 10, 1994<sup>⊗</sup>

The complexes formed by Cu(II) with 1,10-phenanthroline, 5-chloro-1,10-phenanthroline, and 2,9-dimethyl-1,10-phenanthroline were irreversibly adsorbed onto graphite electrodes and examined as electrocatalysts for the reduction of O<sub>2</sub>. Upon reduction, all three complexes catalyze the four-electron reduction of O<sub>2</sub>. The adsorbed complexes with only a single ligand coordinated to the Cu center were much more reactive than those with two coordinated ligands. Analysis of the rising portions as well as the plateaus of current–potential curves recorded at rotating disk electrodes indicated that the coordination of O<sub>2</sub> to the Cu(I) forms of the complexes is the current-limiting step at all potentials. Significant differences exist between the kinetic behavior of the complexes adsorbed on graphite and that of the same complexes dissolved in solution. The electrochemistries and coordination chemistries exhibited by Cu(II) phenanthrolines and Co(II) porphyrins during their electrocatalysis of the reduction of O<sub>2</sub> are compared and contrasted.

Complexes of Cu(II) with 1,10-phenanthroline and related ligands spontaneously adsorb onto graphite electrode surfaces where they serve as active electrocatalysts for the reduction of O<sub>2</sub>. The electrochemical behavior and catalytic reactivities of several complexes of this type have been described in a variety of previous reports.<sup>1–4</sup> The potentials where the adsorbed catalysts function in the reduction of O<sub>2</sub> are close to, or somewhat positive of, the formal potentials of the Cu(II)/Cu(I) couples of the adsorbed complexes and the rates of the catalyzed reduction of O<sub>2</sub> diminish as the structure of the phenanthroline ligand derivatives, L, are varied to make the formal potentials of the CuL<sub>2</sub><sup>2+/+</sup> couples more positive.<sup>2</sup> The reported behavioral patterns are consistent with limitation of the catalytic currents by the rate of formation of an adduct between O<sub>2</sub> and the adsorbed phenanthroline complex of Cu(I). In our previous studies,<sup>1,2</sup> the rates of the catalyzed reductions of O<sub>2</sub> were measured at potentials on the plateaus of current–potential curves recorded with rotating disk electrodes. The electrode potentials were more negative than the formal potential of the adsorbed CuL<sub>2</sub><sup>2+/+</sup> couples, so that the resting state of the adsorbed complexes was Cu(I). In the present study, the rates of the reduction of O<sub>2</sub> were measured on the rising portions as well as on the plateaus of the current–potential curves in order to assess the dependence of the rates on the quantities of the adsorbed complexes which were present in their Cu(I) forms. The results indicate that the current-limiting step is the rate of the reaction between the adsorbed Cu(I) complexes and O<sub>2</sub> molecules from solution to produce an adduct which subsequently accepts electrons from the electrode at a high rate. Evidence to support this mechanistic assignment is provided in this report.

## Experimental Section

**Materials.** The ligands, 1,10-phenanthroline, 5-chloro-1,10-phenanthroline, and 2,9-dimethyl-1,10-phenanthroline, obtained from Aldrich were used as received, as were the other reagent grade chemicals. Complexes were usually prepared in solution by mixing appropriate quantities of ligand with CuSO<sub>4</sub>. However, solutions prepared from salts of the Cu(II)–ligand complex that were isolated as solids and redissolved gave identical results. Solutions were prepared with laboratory deionized water that was further purified by passage through a purification train (Millipore).

**Apparatus and Procedures.** Electrodes were prepared from edge plane pyrolytic graphite and were mounted as previously described<sup>1a</sup> to expose 0.316 cm<sup>2</sup> of the edges of the graphite planes. The mounted electrodes were polished by hand using 600 grit SiC paper followed by sonication for 5 min in pure water. Conventional electrochemical cells and instrumentation were employed. Irreversible adsorption of the complexes of Cu(II) onto the electrode surfaces could be obtained by exposing the polished electrodes to solutions of the complex. Alternatively, the ligand was preadsorbed from a copper-free solution and the ligand-coated electrode was exposed to solutions of Cu<sup>2+</sup>.<sup>1,2</sup> Both procedures produced the same results. Potentials were measured and are quoted with respect to a saturated calomel electrode. Experiments were conducted at the ambient laboratory temperature, 22 ± 2 °C.

## Results

The complexes of Cu<sup>2+</sup> with 1,10-phenanthroline (phen), 5-chloro-1,10-phenanthroline (Cl-phen), and 2,9-dimethyl-1,10-phenanthroline (DMP) were irreversibly adsorbed onto graphite electrodes and examined as catalysts for the electroreduction of O<sub>2</sub> (and H<sub>2</sub>O<sub>2</sub>). Previous studies have described aspects of the electrocatalytic behavior of CuL<sub>2</sub><sup>2+</sup> and CuL<sup>2+</sup> complexes for L = phen and DMP.<sup>2–4</sup> The present study includes experiments for the case where L = Cl-phen and concentrates on the previously unexplored behavior of the adsorbed complexes at potentials on the rising portions of the current–potential curves obtained during the catalyzed reduction of O<sub>2</sub>.

**Cyclic Voltammetric Behavior of Dissolved and Adsorbed Cu(phen)<sub>2</sub><sup>2+</sup>, Cu(Cl-phen)<sub>2</sub><sup>2+</sup> and Cu(DMP)<sub>2</sub><sup>2+</sup>.** At pH 5.2 the cyclic voltammetry of 1 mM solutions of these three complexes at glassy carbon electrodes, where adsorption is weak, consists of a single reversible wave from which formal

\* To whom correspondence should be addressed.

<sup>§</sup> Contribution No. 8944.

<sup>⊗</sup> Abstract published in *Advance ACS Abstracts*, September 15, 1994.

- (1) (a) Zhang, J. J.; Anson, F. C. *J. Electroanal. Chem. Interfacial Electrochem.* **1991**, *341*, 232. (b) *J. Electroanal. Chem. Interfacial Electrochem.* **1993**, *348*, 81.
- (2) Zhang, J. J.; Anson, F. C. *Electrochim. Acta* **1993**, *38*, 2423.
- (3) Sugiyama, K.; Aoki, K. *J. Electroanal. Chem. Interfacial Electrochem.* **1989**, *262*, 211.
- (4) Tarasevich, M. R.; Vol'pin, M. E.; Bogdanovskaya, A.; Orlov, S. B.; Novodarova, G. N.; Kolosova, E. M. *Elektrokhimiya* **1981**, *17*, 1327.

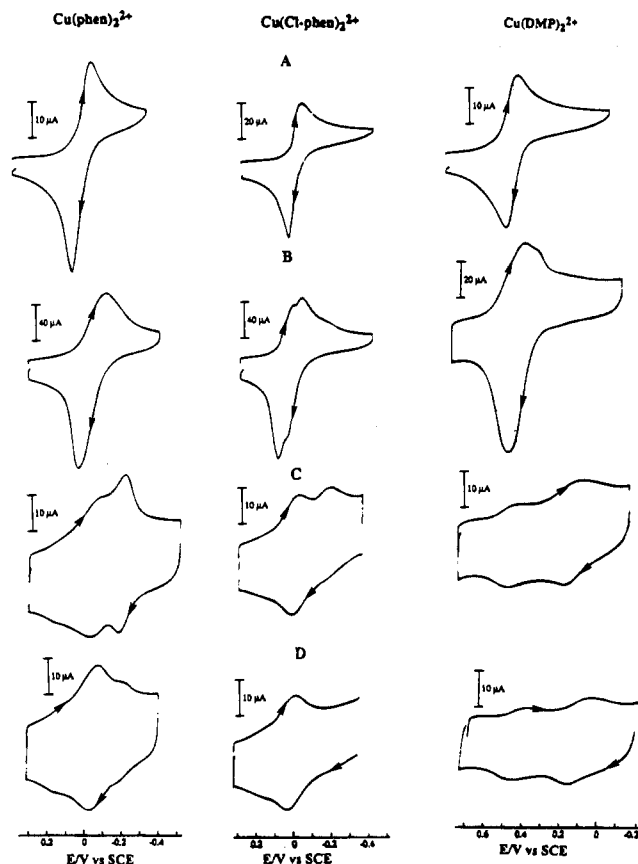


**Figure 1.** Cyclic voltammetry of  $\text{Cu}(\text{phen})_2^{2+}$ ,  $\text{Cu}(\text{Cl-phen})_2^{2+}$  and  $\text{Cu}(\text{DMP})_2^{2+}$ : (A) voltammogram of 1 mM complex, glassy carbon electrode; (B) repeat of (A) at an edge plane pyrolytic graphite electrode (EPG); (C) voltammogram recorded after the EPG electrode used in (B) was transferred to a pure supporting electrolyte solution; (D) repeat of (C) after the electrode was exposed for 10 s to a  $10^{-5}$  M solution of the free ligand and transferred back to the pure supporting electrolyte. Supporting electrolyte: (A, B) 0.04 M Britton–Robinson buffer at pH 5.2; (C, D) buffer as in (A, B) plus 0.1 M  $\text{NaClO}_4$  to diminish the solubility of the complexes. Scan rate =  $50 \text{ mV s}^{-1}$  throughout.

potentials of  $-0.06 \text{ V}$  ( $\text{Cu}(\text{phen})_2^{2+/+}$ ),  $0.015 \text{ V}$  ( $\text{Cu}(\text{Cl-phen})_2^{2+/+}$ ), and  $0.34 \text{ V}$  ( $\text{Cu}(\text{DMP})_2^{2+/+}$ ) were estimated (Figure 1A). The values for the  $\text{Cu}(\text{phen})_2^{2+/+}$  and  $\text{Cu}(\text{DMP})_2^{2+/+}$  complexes agree with previously reported values.<sup>2–4</sup> If edge plane pyrolytic graphite electrodes (EPG) are employed instead of glassy carbon, the stronger adsorption of the complexes produces some distortions in the voltammograms recorded with 1 mM solutions, and the response includes a clear second peak with the Cl-phen ligand and a cathodic shoulder with the DMP ligand (Figure 1B). If the EPG electrodes are transferred to pure supporting electrolyte solutions after exposure to the solutions of the copper complexes, the cyclic voltammograms obtained from the irreversibly adsorbed complexes contain two cathodic waves with all three complexes (Figure 1C). The waves at the more positive potential correspond to the responses obtained in solutions of the complexes (Figure 1A) and can be assigned to the  $[\text{Cu}(\text{phen})_2^{2+/+}]_{\text{ads}}$ ,  $[\text{Cu}(\text{Cl-phen})_2^{2+/+}]_{\text{ads}}$ , and  $[\text{Cu}(\text{DMP})_2^{2+/+}]_{\text{ads}}$  couples. The waves at the more negative potential are assigned to the  $[\text{Cu}(\text{phen})^{2+/+}]_{\text{ads}}$ ,  $[\text{Cu}(\text{Cl-phen})^{2+/+}]_{\text{ads}}$ , and  $[\text{Cu}(\text{DMP})^{2+/+}]_{\text{ads}}$  couples because brief exposure of the coated electrodes to dilute solution of the free ligand caused the waves at more negative potentials to diminish as the waves at more positive potentials grew in magnitude (Figure 1D). The same interpretation was offered for the double peaks observed at graphite electrodes coated with  $\text{Cu}(\text{phen})_2^{2+}$  in a recent report.<sup>3</sup> Responses very similar to those shown in

**Table 1.** Formal Potentials of  $\text{Cu}(\text{II})/\text{Cu}(\text{I})$  Complexes in Solution and on the Surface of Edge Plane Pyrolytic Graphite Electrodes

L	$E^f$ , mV vs SCE		
	$[\text{CuL}_2^{2+/+}]_{\text{soln}}^a$	$[\text{CuL}_2^{2+/+}]_{\text{ads}}^b$	$[\text{CuL}^{2+/+}]_{\text{ads}}^b$
phen	$-60 \pm 5$	$-55 \pm 5$	$-190 \pm 5$
Cl-phen	$15 \pm 5$	$10 \pm 5$	$-170 \pm 5$
DMP	$340 \pm 10$	$430 \pm 10$	$105 \pm 10$

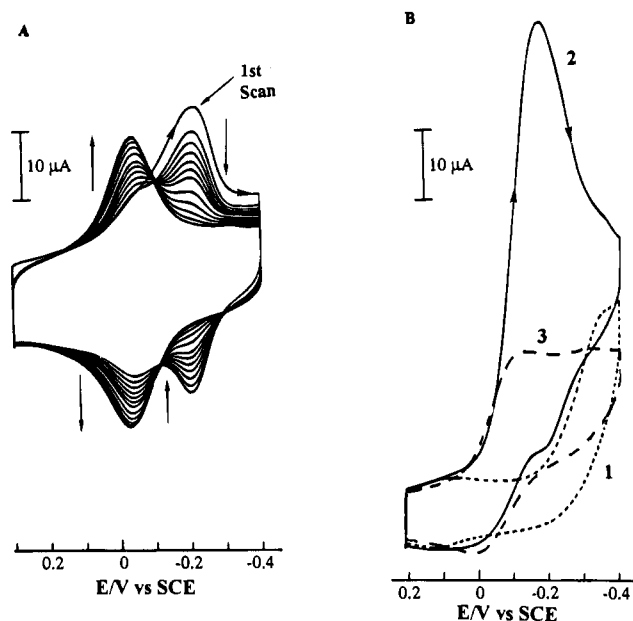
<sup>a</sup> Measured at glassy carbon electrodes. The entries are the average of the values obtained by cyclic and rotating disk voltammetry. Supporting electrolyte: 0.04 M Britton–Robinson buffer at pH 5.2. <sup>b</sup> Measured with the complexes adsorbed on EPG electrodes in pure supporting electrolyte: 0.04 M Britton–Robinson buffer (pH 5.2) + 0.1 M  $\text{NaClO}_4$ .

Figure 1C can also be obtained by preadsorption of the free ligands on pyrolytic graphite electrodes followed by exposure of the electrodes to dilute solutions of  $\text{Cu}^{2+}$ . Thus, the adsorbed ligands can engage in coordination reactions with  $\text{Cu}^{2+}$  ions in solution. However, the presence of two voltammetric waves for surfaces containing mixtures of  $\text{CuL}_2^{2+}$ ,  $\text{CuL}^{2+}$ , and L indicates that the establishment of coordination equilibrium among the adsorbed reactants is slow on the voltammetric time scale. If the equilibration were rapid, only a single voltammetric wave would be observed. That the double peaks shown in Figure 1C persisted even when the potential scan rate was decreased to  $10 \text{ mV s}^{-1}$  demonstrates that the surface coordination equilibria are established slowly. Coordination equilibria are also established slowly in homogeneous solutions containing mixtures of  $\text{Cu}(\text{II})$  with the DMP ligand.<sup>5</sup>

A summary of the formal potentials of the various dissolved and adsorbed copper complexes with the phen, Cl-phen, and DMP ligands is given in Table 1. The formal potentials of the  $[\text{CuL}^{2+/+}]_{\text{ads}}$  couples are of particular interest because it is these singly ligated complexes that exhibit the greatest catalytic activity toward the reduction of  $\text{O}_2$ . Exposure of catalytically active coatings of  $\text{CuL}^{2+/+}$  to solutions of the free ligand, L, diminishes their catalytic activity by converting the adsorbed complexes to their  $\text{CuL}_2^{2+}$  forms. This conversion is demonstrated with the cyclic voltammograms in Figure 2A for the case of  $[\text{Cu}(\text{phen})_2^{2+}]_{\text{ads}}$ . The electrode was coated with  $\text{Cu}(\text{phen})_2^{2+}$  by immersing it for 5 min in a 1 mM solution of phen followed by 5 min in a 1 mM solution of  $\text{Cu}^{2+}$ . The electrode was then transferred to a supporting electrolyte solution containing  $10^{-5}$  M phen, and the series of cyclic voltammograms shown in Figure 2A were recorded by continuous cycling of the electrode potential between 0.4 and  $-0.4 \text{ V}$ . Initially, there was a single voltammetric response near  $-0.21 \text{ V}$ , but with continued cycling this feature diminished as a new peak near  $-0.04 \text{ V}$  developed. The clear “isosbestic points” in the voltammetry (Figure 2A) showed that the initial adsorbed complex was converted to a second adsorbed complex. The formal potential of the final, steady response corresponds to that expected for the  $[\text{Cu}(\text{phen})_2^{2+/+}]_{\text{ads}}$  couple (Table 1). The initial reversible response is therefore assigned to the  $[\text{Cu}(\text{phen})^{2+/+}]_{\text{ads}}$  couple.

The effects of converting  $[\text{Cu}(\text{phen})^{2+/+}]_{\text{ads}}$  to  $[\text{Cu}(\text{phen})_2^{2+/+}]_{\text{ads}}$  on the reduction of  $\text{O}_2$  are shown in Figure 2B. Curve 1 is the voltammetric response for the reduction of  $\text{O}_2$  at the uncoated electrode. The reduction begins near  $-0.2 \text{ V}$ . After  $\text{Cu}(\text{phen})_2^{2+}$  was adsorbed onto the electrode, the reduction of  $\text{O}_2$  shifted to more positive potentials and produced the large peak current shown in curve 2 of Figure 2B. Addition of  $10^{-5}$  M phen to the solution used to record curve 2 caused the  $[\text{Cu}(\text{phen})_2^{2+}]_{\text{ads}}$  to convert to  $[\text{Cu}(\text{phen})_2^{2+/+}]_{\text{ads}}$  (Figure 2A) and produced the

(5) Lei, Y.; Anson, F. C. Experiments in progress, 1994.



**Figure 2.** (A) Cyclic voltammograms recorded during the conversion of  $[\text{Cu}(\text{phen})^{2+}]_{\text{ads}}$  to  $[\text{Cu}(\text{phen})_2^{2+}]_{\text{ads}}$  on a pyrolytic graphite electrode. The electrode was initially coated with  $10^{-9}$  mol  $\text{cm}^{-2}$  of  $[\text{Cu}(\text{phen})^{2+}]_{\text{ads}}$  and transferred to a supporting electrolyte solution containing  $10^{-5}$  M phen to record the voltammograms. Scan rate =  $50$   $\text{mV s}^{-1}$ . Supporting electrolyte:  $0.04$  M Britton–Robinson buffer (pH 5.2) +  $0.1$  M  $\text{NaClO}_4$ . (B) Voltammograms recorded during the reduction of  $0.28$  mM  $\text{O}_2$  at a pyrolytic graphite electrode coated with (1) nothing, (2)  $[\text{Cu}(\text{phen})^{2+}]_{\text{ads}}$ , and (3)  $[\text{Cu}(\text{phen})_2^{2+}]_{\text{ads}}$ . Scan rate =  $25$   $\text{mV s}^{-1}$ . Supporting electrolyte: as in (A).

significant diminishment in the  $\text{O}_2$  reduction current shown in curve 3 of Figure 2B, in which the weaker catalysis probably consists of contributions from both  $[\text{Cu}(\text{phen})_2^{2+}]_{\text{ads}}$  and residual  $[\text{Cu}(\text{phen})^{2+}]_{\text{ads}}$ . Essentially similar behavior was obtained with the  $[\text{Cu}(\text{Cl-phen})^{2+/+}]_{\text{ads}}$  and  $[\text{Cu}(\text{Cl-phen})_2^{2+/+}]_{\text{ads}}$  catalysts, and analogous behavior of the  $[\text{Cu}(\text{DMP})^{2+/+}]_{\text{ads}}$  and  $[\text{Cu}(\text{DMP})_2^{2+/+}]_{\text{ads}}$  system was documented in a previous study.<sup>2</sup>

**Catalysis of the Reduction of  $\text{O}_2$  by the Adsorbed Complexes.** To examine the kinetics of the processes by which the adsorbed complexes catalyze the electroreduction of  $\text{O}_2$ , it is instructive to carry out the reduction at rotating disk electrodes. In Figure 3A is shown a set of current–potential curves for the reduction of  $\text{O}_2$  at a rotating EPG disk electrode with  $\text{Cu}(\text{phen})^{2+}$  adsorbed on its surface. Also shown is the cathodic response of the adsorbed catalyst in the absence of  $\text{O}_2$  (lowest curve in Figure 3A).

It is noteworthy that, especially at lower electrode rotation rates, the reduction of  $\text{O}_2$  begins at potentials somewhat more positive than those where a substantial quantity of  $[\text{Cu}(\text{phen})^{2+}]_{\text{ads}}$  is reduced to  $[\text{Cu}(\text{phen})^{+}]_{\text{ads}}$ . This behavior is the expected result when the rate of the reaction between the reduced catalyst and  $\text{O}_2$  is relatively fast.<sup>6</sup> Levich plots<sup>7</sup> of the plateau currents of the curves in Figure 3A vs the electrode (rotation rate)<sup>1/2</sup> deviate from linearity as the rotation rate increases (Figure 3B). The corresponding Koutecky–Levich plot<sup>8,9</sup> in Figure 3C is parallel to the line calculated for the four-electron reduction of  $\text{O}_2$ , showing that the  $[\text{Cu}(\text{phen})^{+}]_{\text{ads}}$  catalyst produces a four- rather than a two-electron reduction of  $\text{O}_2$ .

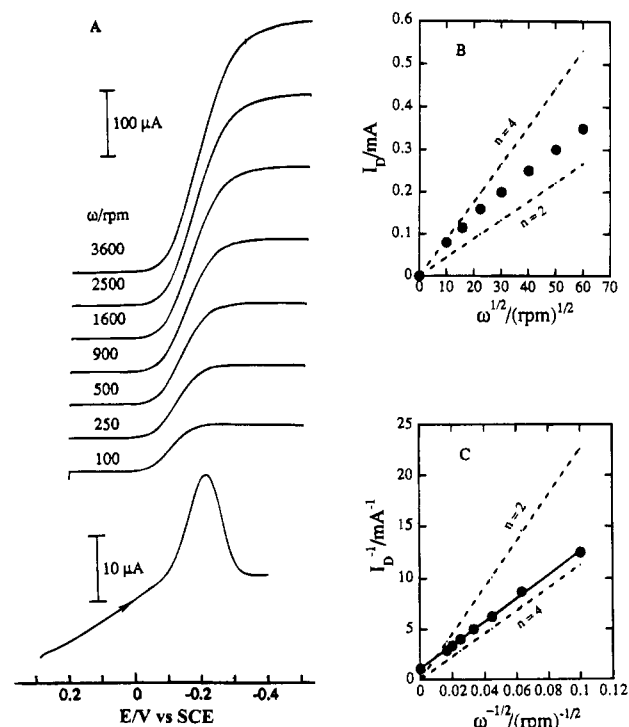


**Figure 3.** Kinetic analysis of the electroreduction of  $\text{O}_2$  as catalyzed by adsorbed  $\text{Cu}(\text{phen})^{2+}$ . (A) Current–potential curves (scan rate =  $10$   $\text{mV s}^{-1}$ ) for the reduction of  $0.28$  mM  $\text{O}_2$  at a rotating edge plane pyrolytic graphite disk electrode on which  $1 \times 10^{-9}$  mol  $\text{cm}^{-2}$  of  $\text{Cu}(\text{phen})^{2+}$  was adsorbed. The lowest curve, recorded at a scan rate of  $50$   $\text{mV s}^{-1}$ , shows the reduction of the adsorbed complex in the absence of  $\text{O}_2$ . (B) Levich plot of the plateau currents from (A) (●) vs the electrode (rotation rate)<sup>1/2</sup>. (C) Koutecky–Levich plot of the (plateau current)<sup>-1</sup> from (A) vs the electrode (rotation rate)<sup>-1/2</sup>. The dashed lines in (B) and (C) give the calculated responses expected for the diffusion-convection-controlled reduction of  $\text{O}_2$  by two ( $n = 2$ ) or four ( $n = 4$ ) electrons. Supporting electrolyte: as in Figure 2A.

The reciprocal of the intercept of the Koutecky–Levich plot in Figure 3C defines a potential-independent kinetic current,  $i_k$ , given by eq 1,<sup>6</sup> where  $n = 4$  for the four-electron reduction,  $F$

$$i_k = nFAk\Gamma_{\text{cat}}C_{\text{O}_2} \quad (1)$$

is the Faraday constant,  $A$  is the electrode area,  $k$  is a second-order rate constant,  $\Gamma_{\text{cat}}$  is the total quantity of catalyst present on the electrode surface, and  $C_{\text{O}_2}$  is the concentration of  $\text{O}_2$  in the solution. Data similar to those for the  $[\text{Cu}(\text{phen})^{2+}]_{\text{ads}}$  catalyst in Figure 3 were also obtained for  $[\text{Cu}(\text{Cl-phen})^{2+/+}]_{\text{ads}}$  and  $[\text{Cu}(\text{DMP})^{2+/+}]_{\text{ads}}$ . The behavior of the  $[\text{Cu}(\text{Cl-phen})^{2+/+}]_{\text{ads}}$  complex is quite similar to that of  $[\text{Cu}(\text{phen})^{2+}]_{\text{ads}}$ , but the  $[\text{Cu}(\text{DMP})^{2+/+}]_{\text{ads}}$  complex is reduced to  $[\text{Cu}(\text{DMP})^{+}]_{\text{ads}}$  at significantly more positive potentials (ca.  $0.1$  V instead of  $-0.1$  V) and the catalyzed reduction of  $\text{O}_2$  also begins at these more positive potentials. However, the rate of the catalyzed reduction, as measured by the magnitude of the plateau current at the rotating disk electrode, is notably smaller with  $[\text{Cu}(\text{DMP})^{2+/+}]_{\text{ads}}$  than with  $[\text{Cu}(\text{Cl-phen})^{2+/+}]_{\text{ads}}$  as catalyst.

Before speculating about the nature of the second-order reaction to which the rate constant in eq 1 applies, it is instructive to examine the rising portion of current–potential curves such as that in Figure 3A. For each catalyst, the onset of the catalytic reduction of  $\text{O}_2$  and the reduction of the adsorbed complex are nearly coincident, which suggests that the latter triggers the former. The quantities of reduced complex present on the electrode surface at potentials on the rising part of the current–potential curves for  $\text{O}_2$  reduction,  $\Gamma_{\text{Cu(I)}}$ , were deter-

(6) Andrieux, C. P.; Saveant, J.-M. In *Molecular Design of Electrode Surfaces*; Murray, R. W., Ed.; John Wiley and Sons, Inc.: New York, 1992; Chapter V.

(7) Levich, V. G. *Physicochemical Hydrodynamics*; Prentice-Hall, Englewood Cliffs, NJ, 1962; pp 345–57.

(8) Koutecky, J.; Levich, V. G. *Zh. Fiz. Khim.* **1956**, *32*, 1565.

(9) Oyama, N.; Anson, F. C. *Anal. Chem.* **1980**, *52*, 1192.

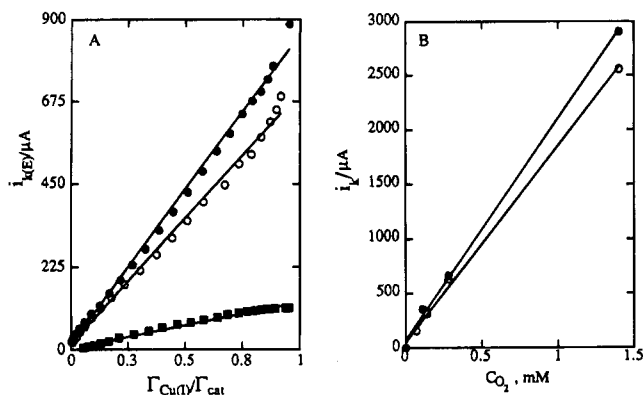


**Figure 4.** (A) Kinetic currents for the electroreduction of  $O_2$  measured on the rising portion of current–potential curves such as those in Figure 3A vs the fraction of the quantities of the  $CuL^{2+}$  complex adsorbed on the electrode surface that is reduced to  $Cu(I)$ . (B) Dependence of the kinetic current obtained from the intercepts of plots such as that in Figure 3C on the concentration of  $O_2$  in the solution: (●) L = phen; (○) L = Cl-phen.

mined by measuring the cathodic areas defined by the voltammetric curves for the reduction of the adsorbed complexes up to each potential of interest in the absence of  $O_2$ . It was determined that the measured areas did not vary significantly as the potential scan rate was varied in the range which produced cathodic peak currents comparable to the largest half-wave currents of the rotating disk voltammograms during the reduction of  $O_2$ . The resulting values of  $\Gamma_{Cu(I)}$  at each potential were plotted against the corresponding currents for the reduction of  $O_2$  when the same electrode was used as a rotating disk. The measured currents,  $i_m$ , were first corrected for the depletion of  $O_2$  at the electrode surface by means of eq 2, where  $i_m$  is the

$$i_k(E) = \frac{i_m i_L}{i_L - i_m} \quad (2)$$

measured current at each potential,  $i_L$  is the calculated Levich current<sup>7</sup> for the diffusion-convection-limited reduction of  $O_2$ , and  $i_k(E)$  is a potential-dependent kinetic current similar to the potential-independent kinetic current in eq 1. In Figure 4A are shown plots of  $i_k(E)$  for the three catalysts vs the fraction of the adsorbed complexes that are reduced to  $Cu(I)$  at potentials on the rising part of the current–potential curves.

The linearity of the plots indicates that the current-limiting reaction is first-order in the quantity of reduced catalyst on the electrode surface. Extrapolation of the plots to  $\Gamma_{Cu(I)}/\Gamma_{cat} = 1$  yielded values of  $i_k(E)$  which were within 10–15% of the values of  $i_k$  obtained from the intercepts of the Koutecky–Levich plots such as the one in Figure 3C. Since these plots were prepared from the plateau currents of current–potential curves like that in Figure 3A where  $\Gamma_{Cu(I)}/\Gamma_{cat} = 1$ , agreement between the two intercepts was to be expected. The behavior shown in Figure 4A indicates that  $i_k(E)$  is related to  $i_k$  according to eq 3.

$$i_k(E) = i_k \Gamma_{Cu(I)}/\Gamma_{cat} = nFAk\Gamma_{Cu(I)}C_{O_2} \quad (3)$$

The linearity of the Koutecky–Levich plots (e.g., Figure 3C) for all three catalysts implies that the current-limiting reaction is first-order with respect to  $O_2$  as was previously reported for the  $[Cu(DMP)^{2+}]_{ads}$  catalyst.<sup>2</sup> This feature was confirmed for the other two catalysts by preparing Koutecky–Levich plots of plateau currents measured in solutions of varying concentrations of  $O_2$ . The values of  $i_k$  obtained from the reciprocal intercepts of the Koutecky–Levich plots increase linearly with the concentration of  $O_2$  as shown in Figure 4B.

**Table 2.** Rate Constants Evaluated for Reaction 5 in Scheme 1

L	$10^{-4}k,^a M^{-1} s^{-1}$	$10^{-4}k,^b M^{-1} s^{-1}$	$10^{-4}k,^c M^{-1} s^{-1}$
phen	$4.4 \pm 0.6$	$3.0 \pm 0.6$	$4.0 \pm 1.0$
Cl-phen	$3.0 \pm 0.5$	$2.5 \pm 0.5$	$4.0 \pm 1.0$
DMP	$1.0 \pm 0.2$	$1.0 \pm 0.2$	$0.8 \pm 0.2$

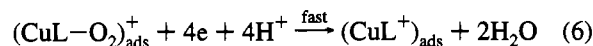
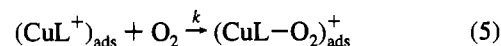
<sup>a</sup> Evaluated from the intercepts of plots such as that in Figure 3C. <sup>b</sup> Evaluated from the slope of plots such as those in Figure 4A. <sup>c</sup> Obtained from best fits of numerically calculated to experimental cyclic voltammograms as in Figure 6.

The slopes of the lines in Figure 4A can be used to obtain estimates of the rate constants in eqs 1 and 3. The values obtained, assuming a four-electron reduction, are listed in Table 2. The rate constants obtained for the  $[Cu(DMP)^{2+}]_{ads}$  catalyst were 3- to 4-fold smaller than the values obtained in a previous study.<sup>2</sup> This difference may be the result of differences in the pyrolytic graphite and the way it was polished in the two studies. Polishing with alumina, as in the previous study, produced surfaces that exhibited less reproducible adsorptive behavior than the surfaces obtained with procedures employed in the present study.

## DISCUSSION

The reaction to which we believe the rate constants in Table 2 should be assigned is reaction 5 in the general mechanism for the catalytic process depicted in Scheme 1.

### Scheme 1



The first-order dependence of the kinetic current on the quantity of  $Cu(I)$  generated in the adsorbed coating (Figure 4A) requires that reduction of the adsorbed  $CuL^{2+}$  complex precede the current-limiting step. A simple outer-sphere electron transfer between the adsorbed  $CuL^+$  complex and  $O_2$  is not likely because the bare graphite electrode could provide an electron having the same energy as that in the adsorbed  $Cu(I)$  complex but no reduction of  $O_2$  occurs at the bare electrode at potentials near the formal potentials of the  $(CuL^{2+/+})_{ads}$  couples (Figure 2B, curve 1). Thus, an inner-sphere pathway such as the one shown in Scheme 1 seems called for. Reaction 5 contemplates the coordination of  $O_2$  to the reduced  $(CuL^+)_{ads}$  complex followed by rapid further reduction of the  $O_2$  in the adduct by electrons from the electrode. The electrochemical reduction is believed to proceed with the partially reduced  $O_2$  held on the electrode surface by coordination to the Cu center of the adsorbed complexes because the rate at which the same complexes catalyze the reduction of  $H_2O_2$  is significantly slower than that at which  $O_2$  is converted to  $H_2O$ .<sup>1,2</sup>

Although the linear Koutecky–Levich plots like that in Figure 3 were parallel to the calculated plot for the four-electron reduction of  $O_2$  to  $H_2O$ , a more sensitive assessment of the reaction stoichiometry was made by means of a rotating graphite disk-platinum ring electrode.<sup>10</sup> In the upper part of Figure 5A are shown current–potential curves for the reduction of  $O_2$  at a rotating graphite disk electrode coated with  $[Cu(Cl-phen)^{2+}]_{ads}$ . In the lower part of Figure 5A the corresponding anodic currents at the platinum ring electrode demonstrate that the reduction of

(10) Albery, W. J.; Hitchman, M. L. *Ring-Disk Electrodes*; Clarendon Press: Oxford, U.K., 1971; p 84 ff.

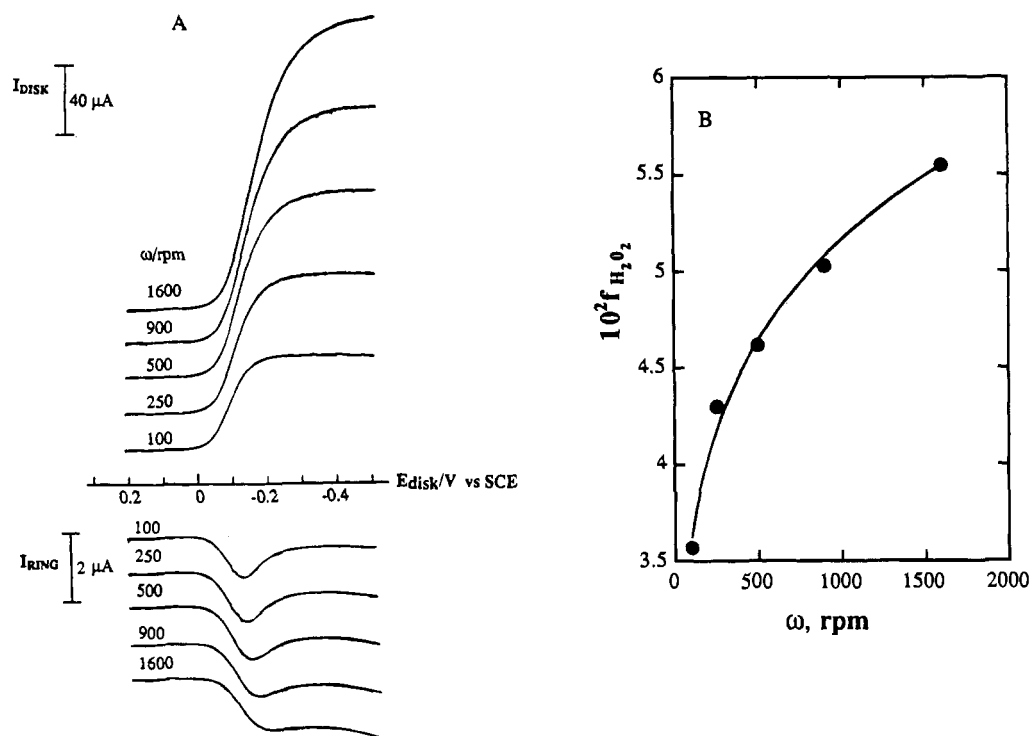


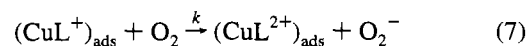
**Figure 5.** (A) Reduction of 0.28 mM  $\text{O}_2$  at a rotating graphite disk-platinum ring electrode (collection efficiency = 0.39) with  $1 \times 10^{-9}$  mol  $\text{cm}^{-2}$  of  $[\text{Cu}(\text{Cl-phen})]^{2+}$  adsorbed on the disk electrode. The platinum ring was maintained at 0.72 V as the disk potential was scanned at 10 mV  $\text{s}^{-1}$ . Supporting electrolyte: as in Figure 2. (B) Fraction of  $\text{O}_2$  that is reduced to  $\text{H}_2\text{O}_2$  on the plateaus of the disk current-potential curves in (A).

$\text{O}_2$  at the disk produces  $\text{H}_2\text{O}_2$  as well as  $\text{H}_2\text{O}$ . The peaked shape of the ring current-disk potential curves at the lower rotation rates reveals that the quantity of  $\text{H}_2\text{O}_2$  produced at the disk diminishes at more negative disk potentials. These results suggest the presence of a parallel catalytic pathway in which  $\text{O}_2$  is reduced to  $\text{H}_2\text{O}_2$  instead of  $\text{H}_2\text{O}$ . The adsorbed Cu complexes are catalytically active toward the electroreduction of  $\text{H}_2\text{O}_2$ , but somewhat more negative potentials are required and the catalytic rates are significantly lower. At low rotation rates some of the  $\text{H}_2\text{O}_2$  is reduced near  $-0.1$  V before it diffuses out of the Levich layer at the surfaces of the disk and ring electrodes so the ring current decreases at potentials more negative than ca.  $-0.1$  V. At higher rotation rates  $\text{H}_2\text{O}_2$  can escape from the thinner Levich layer before it can be reduced, so a steady ring current is obtained from which the extent of  $\text{H}_2\text{O}_2$  production at the disk can be determined. In Figure 5B the fraction of  $\text{O}_2$  that is reduced to  $\text{H}_2\text{O}_2$  (instead of  $\text{H}_2\text{O}$ ) at  $-0.3$  V is plotted as a function of the electrode rotation rate. Most of the  $\text{O}_2$  is reduced to  $\text{H}_2\text{O}$  at all rotation rates, but the fraction of  $\text{O}_2$  that escapes reduction beyond  $\text{H}_2\text{O}_2$  approaches 6% at the highest rotation rates employed. Coatings of the  $[\text{Cu}(\text{phen})^{2+}]_{\text{ads}}$  and  $[\text{Cu}(\text{DMP})^{2+}]_{\text{ads}}$  catalysts led to the production of similar quantities of  $\text{H}_2\text{O}_2$  during the catalyzed reduction of  $\text{O}_2$ .

The behavior shown in Figure 5 could complicate the interpretation of current-potential curves for the reduction of  $\text{O}_2$  at catalyst-coated rotating disk electrodes because of the evident presence of at least two reaction pathways. Fortunately, the fraction of  $\text{O}_2$  that is reduced to  $\text{H}_2\text{O}_2$  instead of to  $\text{H}_2\text{O}$  was small under all of the experimental conditions employed, so we adopted the simplifying assumption that the single, four-electron pathway indicated in Scheme 1 dominated the kinetics. The reciprocal intercepts of the plots like the one in Figure 3C were then used to evaluate rate constants for reaction 5 of Scheme 1 for the three  $\text{CuL}^{2+}$  complexes. The results are summarized in Table 2. The rate constants evaluated from the intercepts of Koutecky-Levich plots of the  $\text{O}_2$  reduction

currents measured on the plateaus of the current-potential curves are in good agreement with those evaluated from the currents on the rising part of the current-potential curves that were used to prepare the plots shown in Figure 4A. This agreement indicates that the rate of transfer of electrons from the electrode to the  $(\text{CuL} - \text{O}_2)_{\text{ads}}^+$  adduct does not limit the  $\text{O}_2$  reduction current at any point of the current-potential curves. The current is limited instead by the rate of formation of the  $(\text{CuL} - \text{O}_2)_{\text{ads}}^+$  adduct. This rate is potential-dependent on the rising part of the current-potential curves because the quantity of  $(\text{CuL}^+)_{\text{ads}}$  changes with potential (see the lowest curve in Figure 3). With the  $[\text{Cu}(\text{phen})^{2+}]_{\text{ads}}$  and  $[\text{Cu}(\text{Cl-phen})^{2+}]_{\text{ads}}$  complexes, the  $\text{O}_2$  reduction currents at electrode rotation rates below ca. 900 rpm reach their potential-independent plateau values before all of the  $(\text{CuL}^{2+})_{\text{ads}}$  is reduced to  $(\text{CuL}^+)_{\text{ads}}$  (Figure 3A). However, these plateau currents are essentially equal to the Levich currents for the four-electron reduction of  $\text{O}_2$  (Figure 3B). The  $[\text{Cu}(\text{phen})^+]_{\text{ads}}$  and  $[\text{Cu}(\text{Cl-phen})^+]_{\text{ads}}$  complexes are apparently sufficiently reactive toward  $\text{O}_2$  for the diffusion-convection-limited reduction current to be reached when only a portion of the available complex is reduced and participates in the catalysis. With the less reducing and (presumably therefore) less reactive  $[\text{Cu}(\text{DMP})^+]_{\text{ads}}$  complex, essentially all of the adsorbed complex must be reduced to obtain reasonable rates of reduction of  $\text{O}_2$ .

**Simulation of Cyclic Voltammograms.** The high reactivity of the  $[\text{CuL}^+]_{\text{ads}}$  complexes toward  $\text{O}_2$  is evident in the effect of  $\text{O}_2$  on the cyclic voltammograms of the adsorbed catalysts. We simulated cyclic voltammograms for comparison with those obtained experimentally. To do so, it was assumed that the total catalytic current would be 4 times the current calculated for the case in which reaction 5 of Scheme 1 was replaced by the hypothetical reaction



because the dioxygen-containing species produced in reaction

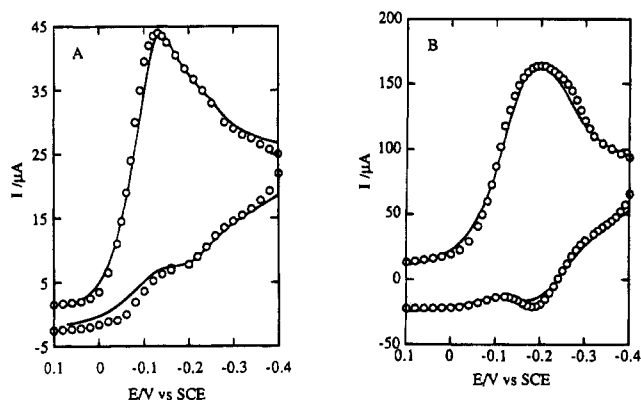


**Figure 6.** Comparison of experimental with numerically simulated cyclic voltammograms for the reduction of 0.28 mM O<sub>2</sub> at electrodes on which  $1.4 \times 10^{-9}$  mol cm<sup>-2</sup> of Cu(phen)<sup>2+</sup> was adsorbed: (A) scan rate = 10 mV s<sup>-1</sup>, interaction parameter<sup>13</sup> = 0.78 (see text); (B) scan rate = 100 mV s<sup>-1</sup>, interaction parameter = 0.70. Solid lines are the calculated responses. The open points are experimental values. The rate constant for reaction 5 (or reaction 7; see text) employed in the simulation was  $4 \times 10^4$  M<sup>-1</sup> s<sup>-1</sup>.

5 or 7 are both assumed to be rapidly converted to H<sub>2</sub>O, by reaction with electrons supplied directly from the electrode in reaction 5 or via reaction with three (CuL<sup>+</sup>)<sub>ads</sub> complexes in reaction 7. The combination of reaction 4 and reaction 7 corresponds to the catalytic case where an otherwise slow electrode process is catalyzed by electron transfer between a substrate and catalyst molecules present in a monolayer on the electrode surface. This case has been analyzed by Andrieux and Saveant<sup>11</sup> and by Aoki et al.<sup>12</sup> By adopting the numerical procedures described by these authors, we calculated the cyclic voltammetric responses shown by the solid lines in Figure 6 for the [Cu(phen)<sup>2+/+</sup>]<sub>ads</sub> catalyst. The value of the rate constant for reaction 7 (and reaction 5) was varied to obtain the best agreement between the calculated and observed voltammetric responses after the former were corrected by adding the estimated contribution from the background charging current. To account for the non-Nernstian voltammetric responses of the catalyst coatings in the absence of O<sub>2</sub>, an interaction parameter was added to the usual equation for the ideal current-potential curve.<sup>13</sup> The interaction parameter was adjusted to obtain the best agreement between the observed and calculated responses of the catalyst coatings in the absence of O<sub>2</sub>, and the same parameter was assumed to apply when O<sub>2</sub> was present. The agreement between the calculated and (corrected) experimental voltammograms in Figure 6 is reasonably good. The rate constant used to obtain the calculated curves in Figure 6 was  $4 \times 10^4$  M<sup>-1</sup> s<sup>-1</sup>. This rate constant is similar to the others in Table 2, which adds support to the values of *k* obtained from the independent measurements. Similar agreement was obtained with simulations of the cyclic voltammetric responses obtained with the [Cu(Cl-phen)<sup>2+/+</sup>]<sub>ads</sub> and [Cu(DMP)<sup>2+/+</sup>]<sub>ads</sub> catalytic systems.

**Comparison with the Behavior of Electrocatalysts Based on Cobalt Porphyrins.** The electroreduction of O<sub>2</sub> is also catalyzed by cobalt porphyrin molecules, CoP, adsorbed on graphite electrodes. Typically, the formal potential of the Co(III)/Co(II) couple of the adsorbed porphyrin is more positive than the potentials where the catalyzed reduction of O<sub>2</sub>

proceeds.<sup>14</sup> As a result, all of the porphyrin is present in its catalytically active, Co(II) form when the reduction of O<sub>2</sub> commences. Therefore, with CoP catalysts, no plots analogous to Figure 4A are relevant. The observed potential dependence of the currents for the reduction of O<sub>2</sub> as catalyzed by adsorbed CoP arises from the potential dependence of the reduction of the (Co<sup>II</sup>P-O<sub>2</sub>)<sub>ads</sub> adduct whose formation on the electrode surface is believed to be the first step in the CoP-catalyzed reduction of O<sub>2</sub>. Although, as with the [CuL<sup>2+/+</sup>]<sub>ads</sub> catalysts examined in this study, the rate of formation of the CoP-O<sub>2</sub> adduct can limit the observed reduction currents under some experimental conditions, the current that would be observed if this rate were infinite can be calculated in the same way that eq 2 is used to calculate the current that would be observed if the electroreduction of O<sub>2</sub> produced no decrease in its concentration at electrode surfaces.<sup>15</sup> Alternatively, the reduction can be inspected at the foot of the current-potential curves where the measured currents are much smaller than the rate with which the CoP-O<sub>2</sub> adduct can be formed. The kinetic currents and corresponding rate constants obtained by either route exhibit a potential dependence: plots of log *i*<sub>k</sub> or log *k* vs *E* have reciprocal slopes that are close to 120 mV per decade.<sup>15</sup>

Application of the same procedure to the current-potential responses obtained with the [CuL<sup>2+/+</sup>]<sub>ads</sub> catalysts leads to a different outcome. The kinetic currents exhibit a potential dependence that can be accounted for entirely by the potential dependence of the quantity of the reduced form of the catalyst that is formed on the electrode surface. When this dependence is accounted for, as in Figure 4A, the kinetic currents or rate constants are not potential dependent; if they were, the plots in Figure 4A would not be linear. Thus, although similar adsorbed catalyst-dioxygen adducts are invoked as intermediates in the mechanisms proposed for the catalyzed reduction of O<sub>2</sub> by both cobalt porphyrins and copper phenanthroline complexes, the two types of catalyst yield current-potential curves that exhibit distinctly different potential dependences on their rising portions. With the Cu(II) complexes, the currents are controlled at all potentials by the rate of formation of a catalyst-O<sub>2</sub> adduct, which depends upon the fraction of the Cu(II) precatalyst that has been converted to its Cu(I) form. Once it has formed, the O<sub>2</sub> in the adsorbed adduct is apparently immediately reduced by electrons from the electrode at potentials on the rising part, as well as the plateaus of the current-potential curves. In the case of cobalt porphyrins, the catalyst-dioxygen adduct is not reduced immediately at potentials on the rising part of the current-potential curves. We know this to be the case because the rate of reduction of O<sub>2</sub> depends upon the electrode potential under conditions where there is no change in the oxidation state of the cobalt center of the adsorbed porphyrin. The currents on the plateaus of the current-potential curves are controlled by the rate of formation of the adducts with both types of catalysts. However, the rate of electron transfer from the electrode to the adduct limits the currents on the rising part of the current-potential curves obtained with CoP but not with CuL<sup>2+/+</sup> as catalyst.

**Comparison with the Reduction of O<sub>2</sub> by Cu(I)-Phenanthroline Complexes in Solution.** The kinetics of the homogeneous redox reactions between various phenanthroline complexes of Cu(I) and O<sub>2</sub> have been examined in several previous studies.<sup>16-20</sup> The most recent results point to an inner-sphere

- (11) Andrieux, C. P.; Saveant, J.-M. *J. Electroanal. Chem. Interfacial Electrochem.* **1978**, *93*, 163.  
 (12) Aoki, K.; Tokuda, K.; Matsuda, H. *J. Electroanal. Chem. Interfacial Electrochem.* **1986**, *199*, 69.  
 (13) Brown, A. P.; Anson, F. C. *Anal. Chem.* **1977**, *49*, 1589.

- (14) Ni, C.-L.; Anson, F. C. *Inorg. Chem.* **1985**, *24*, 4754.  
 (15) Shi, C.; Anson, F. C. *Electrochim. Acta* **1994**, *39*, 1613.  
 (16) Crumbliss, A. L.; Poulos, A. T. *Inorg. Chem.* **1975**, *14*, 1579.  
 (17) Crumbliss, A. L.; Gestaut, L. J. *J. Coord. Chem.* **1976**, *5*, 109.  
 (18) Goldstein, S.; Czapski, G. *J. Am. Chem. Soc.* **1983**, *105*, 7276.  
 (19) Goldstein, S.; Czapski, G. *Inorg. Chem.* **1985**, *24*, 1087.

pathway in which the reduction product,  $\text{H}_2\text{O}_2$ , undergoes further reduction to  $\text{H}_2\text{O}$  much more slowly than it is formed by the reduction of  $\text{O}_2$ .<sup>20</sup> The relative reactivity of the  $\text{CuL}^+$  and  $\text{CuL}_2^+$  complexes in solution has not been addressed specifically, probably because  $\text{Cu}(\text{phen})^+$  and  $\text{Cu}(\text{Cl-phen})^+$ , if formed, would spontaneously decompose to form the corresponding  $\text{CuL}_2^+$  complex and  $\text{Cu}^+$ . High reactivity is observed under conditions where the  $\text{Cu}(\text{phen})_2^+$  and  $\text{Cu}(\text{Cl-phen})_2^+$  complexes are the predominant species present in solution, but the possibility that more than a single geometric isomer may be involved in electron transfer reactions involving  $\text{Cu}(\text{I})$  and  $\text{Cu}(\text{II})$  complexes always needs to be considered.<sup>21</sup> Stable solutions containing both the  $\text{Cu}(\text{DMP})^+$  and the  $\text{Cu}(\text{DMP})_2^+$  complexes can be prepared, but only the  $\text{Cu}(\text{DMP})^+$  is oxidized by  $\text{O}_2$  at a significant rate.<sup>5</sup>

With the copper phenanthroline complexes present only on the electrode surface, the kinetic situation is different. An inner-sphere catalytic pathway seems unambiguously called for to account for the ability of the adsorbed  $\text{CuL}^+$  complexes to cause  $\text{O}_2$  to be reduced at electrode potentials where the bare electrode itself is inert. The lesser catalytic activity of the  $(\text{CuL}_2^+)_{\text{ads}}$  complexes may reflect the greater difficulty faced by the adsorbed complexes in altering their coordination sphere by expansion or isomerization when the electrode surface poses a steric barrier to the coordination of incoming ligands. In addition, the functional groups on the surface of graphite electrodes may compete with incoming ligands for coordination sites on the copper center. Presumably, the less coordinatively encumbered  $(\text{CuL}^+)_{\text{ads}}$  complexes could more readily accommodate the entry of an  $\text{O}_2$  molecule into the coordination sphere of the copper center to initiate the inner-sphere reaction pathway.

The double voltammetric peaks exhibited by the adsorbed complexes in Figure 1C have no counterparts in the solution electrochemistry of  $\text{Cu}(\text{phen})_2^{2+}$  or  $\text{Cu}(\text{Cl-phen})_2^{2+}$ . Voltammograms of these complexes, which are the predominant species present in solutions containing equimolar quantities of  $\text{Cu}^{2+}$  and the ligands, do not resemble those in Figure 1C; a single wave for the one-electron reduction of the complexes appears at potentials very close to those where the two-electron reduction to  $\text{Cu}$  metal occurs, and it is very difficult to separate the two processes. In any case, the reduction of  $\text{CuL}_2^{2+}$  is expected to consume only 0.5 electron per  $\text{Cu}(\text{I})$  center and to produce equimolar quantities of  $\text{CuL}_2^+$  and  $\text{Cu}^{2+}$  on the basis of the equilibrium constants for the formation of the  $\text{Cu}(\text{II})$  and  $\text{Cu}(\text{I})$  complexes.<sup>22</sup> Thus, the homogeneous reduction of  $\text{O}_2$  may well be accomplished by  $\text{CuL}_2^+$  even in solutions in which  $\text{CuL}_2^{2+}$

is the predominant oxidized form of the copper complex. The fact that separated voltammetric responses for the  $\text{CuL}_2^{2+/+}$  and  $\text{CuL}_2^{2+/+}$  couples ( $\text{L} = \text{phen}, \text{Cl-phen}$ ) can be obtained for the adsorbed but not for the dissolved complexes reflects the very significant influence that adsorption has on the coordination chemistry of the complexes. The surfaces of pyrolytic graphite electrodes not only serve as a convenient substrate on which to adsorb precatalysts but also can alter coordination rates and/or equilibria in ways that are kinetically advantageous.

The more positive formal potentials of the  $\text{Cu}^{2+}$  complexes with DMP allow their electrochemistry to be observed in solution without interference from the deposition of  $\text{Cu}^0$ . Two cathodic waves are observed under conditions where both  $\text{Cu}(\text{DMP})_2^{2+}$  and  $\text{Cu}(\text{DMP})_2^{2+}$  are present in solution, but significant catalytic activity toward the reduction of  $\text{O}_2$  is evident only at the wave corresponding to the  $\text{Cu}(\text{DMP})_2^{2+/+}$  couple.<sup>5</sup> The lack of reactivity toward  $\text{O}_2$  of the  $\text{Cu}(\text{DMP})_2^+$  complex in solution can be understood in terms of the much more positive formal potential of the  $[\text{Cu}(\text{DMP})_2^{2+/+}]_{\text{soln}}$  couple compared with the  $[\text{Cu}(\text{phen})_2^{2+/+}]_{\text{soln}}$  and  $[\text{Cu}(\text{Cl-phen})_2^{2+/+}]_{\text{soln}}$  couples (Table 1). The even more positive formal potential of the  $[\text{Cu}(\text{DMP})_2^{2+/+}]_{\text{ads}}$  couple makes the lack of reaction of  $[\text{Cu}(\text{DMP})_2^+]_{\text{ads}}$  with  $\text{O}_2$  understandable.<sup>2</sup>

The ability of the adsorbed, but not the dissolved, complexes examined in this study to produce rapid four-electron reductions of  $\text{O}_2$  seems most likely to result from the ability of the electrode to supply as many electrons as the reactive, partially reduced intermediates generated on the electrode surface can consume. With homogeneous solutions of the reactants, the partially reduced dioxygen bound to the catalytically activating copper center may dissociate before it encounters the additional  $\text{CuL}_2^+$  complexes that must deliver the electrons needed for the reduction to continue. When to this factor is added the more negative formal potentials of the  $[\text{CuL}_2^{2+/+}]_{\text{ads}}$  couples (Table 1), it is not difficult to understand the significant differences between the adsorbed and dissolved copper complexes in both the rates and the stoichiometry of the reductions of  $\text{O}_2$  that they catalyze. What remains to be explained are the factors underlying the enhanced susceptibility toward reduction that  $\text{O}_2$  molecules experience upon coordination to either copper(I)-phenanthroline or cobalt(II)-porphyrin complexes.

**Acknowledgment.** This work was supported in part by the National Science Foundation and by a grant from the ONR/DARPA. Frequent discussions with Dr. Chunnian Shi and Dr. Beat Steiger were stimulating and helpful. We are indebted to Dr. Yuanwu Xie for the simulation program on which Figure 6 is based, and we are grateful to Prof. J.-M. Savéant and his group for supplying annotated copies of programs applicable to the simulation of cyclic voltammograms for electrocatalytic systems.

(20) Goldstein, G.; Czapski, G.; van Eldik, R.; Cohen, H.; Meyerstein, D. *J. Phys. Chem.* **1991**, *95*, 1282.

(21) Meagher, N. E.; Juntunen, K. L.; Salki, C. A.; Ochrymowycz, L. A.; Rorabacher, D. B. *J. Am. Chem. Soc.* **1992**, *114*, 10411 and references therein.

(22) McBryde, W. A. E. *A Critical Review of Equilibrium Data for Proton and Metal Complexes of 1,10-Phenanthroline and 2,2'-Bipyridyl and Related Compounds*; Pergamon Press: New York, 1978.